Arch. Biol. Sci., Belgrade, 61 (4), 703-711, 2009 DOI:10.2298/ABS0904703L

NEURAL DIFFERENTIATION OF ADIPOSE-DERIVED STEM CELLS BY INDIRECT CO-CULTURE WITH SCHWANN CELLS

XIAOJIE LI[1], DAPENG LIAO[1], PING GONG[2], QUAN YUAN[1], and ZHEN TAN[2]

[1]*State Key Laboratory of Oral Diseases, West China College of Stomatology, Sichuan University,* 610041 Chengdu, China
[2]*Dental Implant Center, West China College of Stomatology, Sichuan University,* 610041 Chengdu, China

Abstract — To investigate whether adipose-derived stem cells (ADSCs) could be subject to neural differentiation induced only by Schwann cell (SC) factors, we co-cultured ADSCs and SCs in transwell culture dishes. Immunoassaying, Western blot analysis, and RT-PCR were performed (1, 3, 7, 14 d) and the co-cultured ADSCs showed gene and protein expression of S-100, Nestin, and GFAP. Further, qRT-PCR disclosed relative quantitative differences in the above three gene expressions. We think ADSCs can undergo induced neural differentiation by being co-cultured with SCs, and such differentiations begin 1 day after co-culture, become apparent after 7 days, and thereafter remain stable till the 14th day.

Key words: Adipose-derived stem cells, Schwann cells, co-culture, neural differentiation

UDC 577.25:616.314-089.843

INTRODUCTION

In 2000, Woodbury et al. were the first to induce bone marrow stromal cells (BMSCs) to differentiate into the neuronal phenotype *in vitro*, expressing neuron-specific enolase, NeuN, neurofilament-M, tau, trKA, and Nestin (Woodbury et al., 2000). Since then, the possibility of obtaining neural cells from BMSCs, as a new biological concept with potential clinical application, has been extensively investigated (Chopp et al., 2002; Hermann et al., 2004; Mahmood et al., 2004; Zurita et al., 2004, 2006; Bossolasco et al., 2005). Bone marrow stromal cells would be an ideal source for nerve tissue engineering if the procedures to harvest them were not so painful and invasive, and if the procedures could yield enough BMSCs more easily (Zuk et al., 2001).

Adipose-derived stem cells (ADSCs) are isolated from adipose tissue, which is derived from embryonic mesoderm. These ADSCs are self-renewable and can differentiate along several mesenchymal tissue lineages, including adipocytes, osteoblasts, myocytes, chondrocytes, endothelial cells, and cardiomyocytes (Zuk et al., 2001; Gimble et al., 2007). Such cells can also be induced into neuro-like cells or a Schwann cell phenotype *in vitro* (Safford et al., 2002; Ning et al., 2006; Kingham et al., 2007), and intra-cerebral transplantation of human ADSCs can improve neurological deficits after cerebral ischemia in rats (Kang et al., 2003). In addition, liposuction is a common and safe surgical procedure, while subcutaneous adipose tissue is abundant, readily accessible, and relatively expendable, so enough ADSCs can be obtained with minimal risk (Fraser et al., 2006). Adipose-derived stem cells seem more suitable than BMSCs for nerve tissue engineering as alternative cell sources of Schwann cells (SCs).

In all methods of inducing BMSC neural differentiation *in vitro*, co-culture seems a simple and effective approach. After performing direct co-culture of SCs and BMSCs, Zurita suggested that intercellular contacts could play an important role in the process of BMSC neural differentiation (Zurita et al., 2005). However, according to previous studies (Ying et al., 2002; Alvarez et al., 2003; Wang et al., 2003; Chen et al., 2006), the possibility of cell fusion cannot be excluded, so Zurita performed indirect co-culture of SCs and BMSCs in transwell culture dishes and proved BMSCs neural differentiation

even if without intercellular contacts (Zurita et al., 2007). This means that only by means of cell factors secreted by SCs, BMSCs can also differentiate into neuro-like cells successfully. But until now, there were no reports about whether ADSCs could realize neural differentiation only by co-culture with SCs. To solve this problem, we applied transparent polycarbonate membranes with pores of 1.0 μm to impede contact between SCs and ADSCs and performed an indirect co-culture, hoping to induce ADSC neural differentiation and investigate the regularity of such differentiation at different time points (1, 3, 7, 14 d) after co-culture.

MATERIAL AND METHODS

All animal experiments described in this report were approved by the Ethical Guideline Committee for Animal Care of West China College of Medical Sciences, Sichuan University.

Isolation, culture, and identification of ADSCs and SCs

Adipose-derived stem cells were isolated from subcutaneous adipose tissue of the inguinal region of adult Sprague-Dawley rats. The subcutaneous fat was carefully dissected and then enzymatically dissociated for 60 min at 37°C using 0.1% (w/v) collagenase type I (Sigma, UK) and passed through a 75-μm filter to remove undissociated tissues, after which it was neutralized by the addition of alpha-Modified Eagle Medium (α-MEM; Hyclone, USA) containing 20% (v/v) fetal bovine serum (FBS, Hyclone, USA) and centrifuged at 1000×g for 8 min. The stromal cell pellet was resuspended in α-MEM containing 20% (v/v) FBS (Hyclone, USA) with 1% (v/v) penicillin/streptomycin solution. Cultures were maintained at subconfluent levels in an incubator at 37°C with 5% CO_2 and passaged with trypsin/EDTA (Sigma, UK) when required.

Schwann cells were isolated from the bilateral sciatic nerves of 1- to 2-day-old Sprague-Dawley rat pups according to previous reports (Zurita et al., 2005) and cultured in α-MEM containing 20% (v/v) FBS (Hyclone, USA) with 2 μM forskolin (Sigma, UK), 20 ng/ml basic fibroblast growth factor (bFGF; PeproTech Ltd., UK), and 1% (v/v) penicillin/streptomycin solution. The culture medium was changed every 72 h.

Adipose-derived stem cells at passage 3 were identified by immunocytochemistry with antibodies against Stro-1, CD90, CD10, CD146, CD44, and CD34 (1:100, Santa Cruz, CA, USA). The multiple differentiation potential of these ADSCs was also investigated as previously described (Kingham et al., 2007). For osteogenic induction, cultures were treated with 100 μg/ml ascorbate, 0.1 μM dexamethasone, and 10 mM β-glycerophosphate for 3 weeks. Cells were then fixed with 4% (w/v) paraformaldehyde for 30 min at room temperature, washed three times with phosphate-buffered saline (PBS), and then incubated with 1% (w/v) Alizarin Red solution to stain for calcium deposition. For adipogenic induction, cells were treated with 0.5 mM isobutylmethylxanthine (IBMX), 1 μM dexamethasone, 10 μM insulin, and 200 μM indomethacin for 3 weeks. Cells were then fixed with 10% (v/v) formalin for 60 min, washed in H_2O, and stained for lipid clusters with Oil Red O. Stem cells were identified in living cultures on the basis of cell soma and nuclear morphology. They were also identified by immunocytochemical labeling for S100 protein with antibody against S100 (1:100, Santa Cruz, CA, USA). The cover slips were examined using an Olympus IX 70 inverted fluorescence microscope.

Co-culture of ADSCs and SCs

To co-culture ADSCs and SCs, we used transwell culture dishes with a polycarbonate membrane (Millipore, USA). The pore size of membranes in our experiment was 1.0 μm, which is much smaller than size of the ADSC body (approximately 80-160 μm) and therefore greatly inhibits the migration of ADSCs into the lower chamber. Schwann cells (6×10^4 cells/cm^2, in 3 ml of culture medium) were cultured in the well, and ADSCs (3×10^4 cells/cm^2) were cultured on the permeable membrane support, with co-cultures maintained in α-MEM containing 20% (v/v) FBS, so that both types of cells were exposed to the same culture media conditions, without cell contacts (Zurita et al., 2007). Meanwhile, ADSCs cultured on the permeable membrane support without SCs in the lower chamber were taken as

control groups. At different time points (1, 3, 7, 14 d) after co-culture, all the membranes were cut down from the insert and mounted on glass cover slips for immunostaining.

Immunoassaying and Western blotting

For immunoassaying, cells were cultured on glass cover slips for 24 h and fixed in 4% (w/v) paraformaldehyde in phosphate-buffered saline (PBS, pH 7.5) for 30 min, washed with PBS thoroughly and treated with 3% (v/v) H_2O_2 for 5 min, incubated for 1 h with blocking buffer [5% (w/v) normal goat serum (Sigma, UK)/0.1% (w/v) TritonX-100 in PBS, pH 7.5], then incubated with primary antibodies, including mouse antibodies against S100 (1:100, Santa Cruz, USA), glial fibrillary acidic protein (GFAP) (1:200, Santa Cruz), Nestin (1:100, Santa Cruz), Stro-1 (1:100, Santa Cruz), CD90 (1:100, Santa Cruz), CD10 (1:100, Santa Cruz), CD146 (1:100, Santa Cruz), CD44 (1:100, Santa Cruz), and CD34 (1:100, Santa Cruz) at 4°C overnight. After thorough washing, the cover slips were incubated with secondary biotinylated antibodies and horseradish peroxide-conjugated streptavidin. The peroxidase reaction was developed using 3, 30-diaminobenzidine tetrahydrochloride (DAB) as chromogen. The cells were counterstained with hematoxylin and then examined using an Olympus IX 70 inverted phase contrast microscope (Olympus, JAPAN). Stro-1 and anti-mouse fluorescein isothiocyanate (FITC)-conjugated secondary antibody (1:100, Santa Cruz) were used to label ADSCs, after which fluorescence signals were detected at emission wavelength of 488/522 nm (FITC, green) with an Olympus IX 70 inverted phase contrast fluorescence microscope (Olympus, JAPAN).

Protein from co-cultured ADSCs and ADSCs of control groups was extracted with a commercially available protein assay kit (Bio-Rad, UK). After determination of protein concentrations, 20 μg of the protein was mixed with an equal amount of 2 × sodium dodecyl sulfate (SDS) loading buffer for Western blot analysis as previously reported (Kingham et al., 2007). Proteins were denatured at 99°C for 5 min, then resolved at 120 V on 15% (for S100) or 10% (for GFAP and Nestin) sodium dodecyl sulfate polyacrylamide gels. Following electrophoretic transfer to polyvinylidene difluoride membranes, membranes were blocked for 1 h in 5% (w/v) non-fat dry milk in TBS-Tween (10 mM Tris pH 7.5, 100 mM NaCl, 0.1% (v/v) Tween). The membranes were then incubated overnight at 4°C with primary antibodies, including mouse antibodies to S100 (1:200, Santa cruz, CA, USA), mouse antibodies to nestin (1:200, Santa Cruz, USA), mouse antibodies to GFAP (1:200, Santa Cruz, USA), and GAPDH (1:500, Santa Cruz, USA). After washing with TBS-Tween, membranes were incubated with horseradish peroxidase-conjugated secondary antibody (goat anti-mouse, 1:1000; Santa Cruz, USA) at room temperature for 1 h. The loading control was GAPDH antibody. The blots were developed via enhanced chemiluminescence (Pierce, Rockford, IL, USA) and were digitally scanned (Bio-Rad, CA, USA).

RNA reverse transcriptase polymerase chain reaction (RT-PCR) and quantitative real-time PCR (qRT-PCR) analysis

Total RNA was extracted from all of the specimens at different time points (1, 3, 7, 14 d) using the Trizol Reagent (Invitrogen, USA) according to the manufacturer's instructions. The yield and quality of the RNA were assessed by measuring the absorbance at 260 and 280 nm, followed by electrophoresis on 3% (w/v) agarose gels. Total RNA (500 ng) was reverse-transcribed into complementary DNA (cDNA) with the PrimeScriptTM RT Reagent Kit (Perfect Real Time, Takara, Japan) according to the manufacturer's guidelines. Primers of S100, GFAP, Nestin, and the internal calibrator [glyceraldehyde-3-phosphate dehydrogenase (GAPDH) (synthesized by Takara Biological Technology Co. Ltd, Dalian, China)] are listed in Table 1. A 25-μl PCR reaction solution (2×SYBR Premix Ex TaqTM 12.5 μl; 10 μmol/l forward primer 0.5 μl; 10 μmol/l reverse primer 0.5 μl; 50×ROX Reference Dye1 0.5 μl, cDNA 2 μl; and dH_2O 9 μl) was amplified in the Applied Biosystems 7300 Real-Time PCR System (ABI, USA). The thermocycle of the PCR reaction was as follows: after an initial denaturation at 95°C for 10 s, 45 cycles of denaturation at 95°C for 5 s and annealing at 60°C for 31 s were performed. The PCR products went through agarose-gel electrophoretic analysis (BIO-

Table 1. Primer sets for RT-PCR and quantitative real-time PCR analysis. For. and Rev. indicate forward and reverse primers, respectively. All primers were purchased from Takara Biological Technology Co. Ltd, (Dalian, China).

Gene	Primer sequences (5'-3')	Product size (bp)	Annealing temperature (°C)	GenBank accession No.
S-100	For.: ctgccaaaacaggatctcagc Rev.: cttgttcagggtgtcaggatgt	101	62.4	L18948
NESTIN	For.: agaagctgggtctgaagcacta Rev.: gggagtagagtcagggagagttt	148	58.3	NM012987
GFAP	For.: gagggacaatctcacacaggac Rev.: gactcaaccttcctctccagat	156	62.4	NM017009
GAPDH	For.: tatgactctacccacggcaagt Rev.: atactcagcaccagcatcacc	138	61.8	NW047717

RAD, USA). During the real-time PCR process, the fluorescence signal was collected during annealing steps. The value of Ct (cycle of threshold) was calculated for further statistical analysis. In order to examine the efficiency of real-time PCR, standard curves were established with serial dilution of sample RNA (500 ng; S100, GFAP, Nestin, GAPDH, 10 × dilution). Total RNA of ADSCs in control groups was taken as a non-template control, which was included in all experiments and performed with RT-PCR to evaluate DNA contamination of reagents used for amplification. None of the experiments resulted in a positive signal from the non-template controls.

Statistical analyses

All data were expressed as the mean ± SEM. Statistical calculations were performed using the SPSS software (SPSS, Chicago, IL, USA). Inter-group comparisons were made by one-way analysis of variance (ANOVA), after which Tukey's honestly significant difference test (Tukey HSD) was adopted to perform multiple inter-group comparisons. Values of P less than 0.05 were considered to be significant.

RESULTS

Immunocytochemical assessment of ADSC stem cell markers showed positive for Stro-1, CD90, CD10, CD146, and CD44, but totally negative for CD34 (Fig. 1). As there were no specific markers, ADSCs were identified on the basis of a complex immune phenotype characterized by the lack of a hematopoietic stem cell marker such as CD34 and expression of a number of surface molecules, including CD90, CD10, CD146, CD44, and STRO-1 (Ning et al., 2006; Krampera et al., 2007). To investigate the mul-

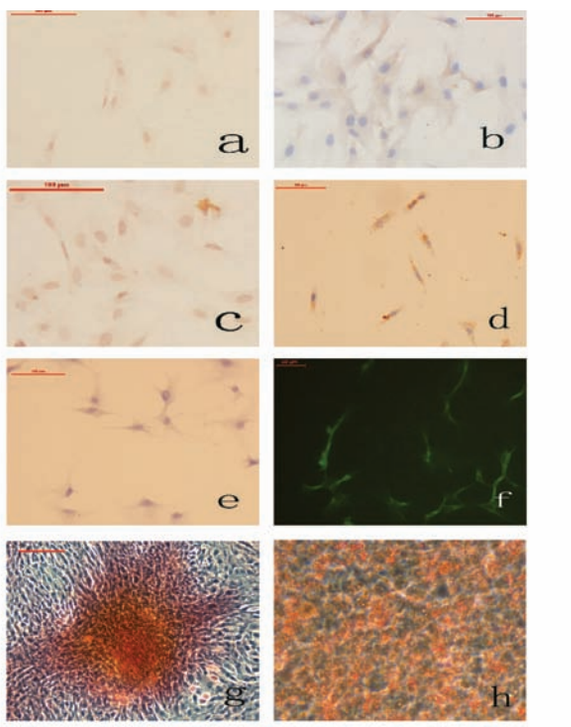

Fig. 1. Identification of ADSCs. Immunocytochemical assessments of ADSC stem cell markers: a. CD90 (+), b. CD10 (+), c. CD44 (+), d. CD146 (+), e. CD34 (-), f. Stro-1(+), g. Alizarin red staining showed some mineralized nodule formation in ADSCs cultures, h. cultured ADSCs formed Oil Red O-positive lipid clusters. Scale bar = 100 μm (a, b, c, d, e, g, h); scale bar = 50 μm (f).

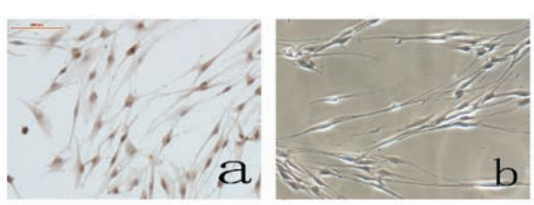

Fig. 2. Identification of SCs.a. Immunocytochemical assessment of Schwann cells showing positive for S100 protein, b. morphology of Schwann cells under phase contrast microscope showing typical elongated spindle shape. Scale bar = 100 μm.

tiple differentiation potential of cells isolated from subcutaneous adipose tissue, they were treated with agents known to induce differentiation into osteoblastic and adipogenetic phenotypes. Osteogenic differentiation was confirmed by the production of calcium deposits detected with Alizarin Red (Fig. 1) and adipogenic differentiation by the presence of Oil Red O-positive lipid clusters (Fig. 1). With respect to morphology, SCs under a phase contrast microscope had a typical elongated spindle shape, and immunocytochemical assessment showed positive for S100 protein with high purity (Fig. 2).

The morphology of co-cultured ADSCs began to change as early as 24 h after co-culture, showing the elongated spindle shape characteristic of SCs, and co-cultured ADSCs with that shape became more and more numerous with the passage of time. Nestin protein is a neural progenitor cell marker, while both S-100 and GFAP protein are glial markers; they are all cell markers for identifying SCs (Ning et al., 2006; Kingham et al., 2007). Our immunocytochemical assessment of co-cultured ADSCs showed positive

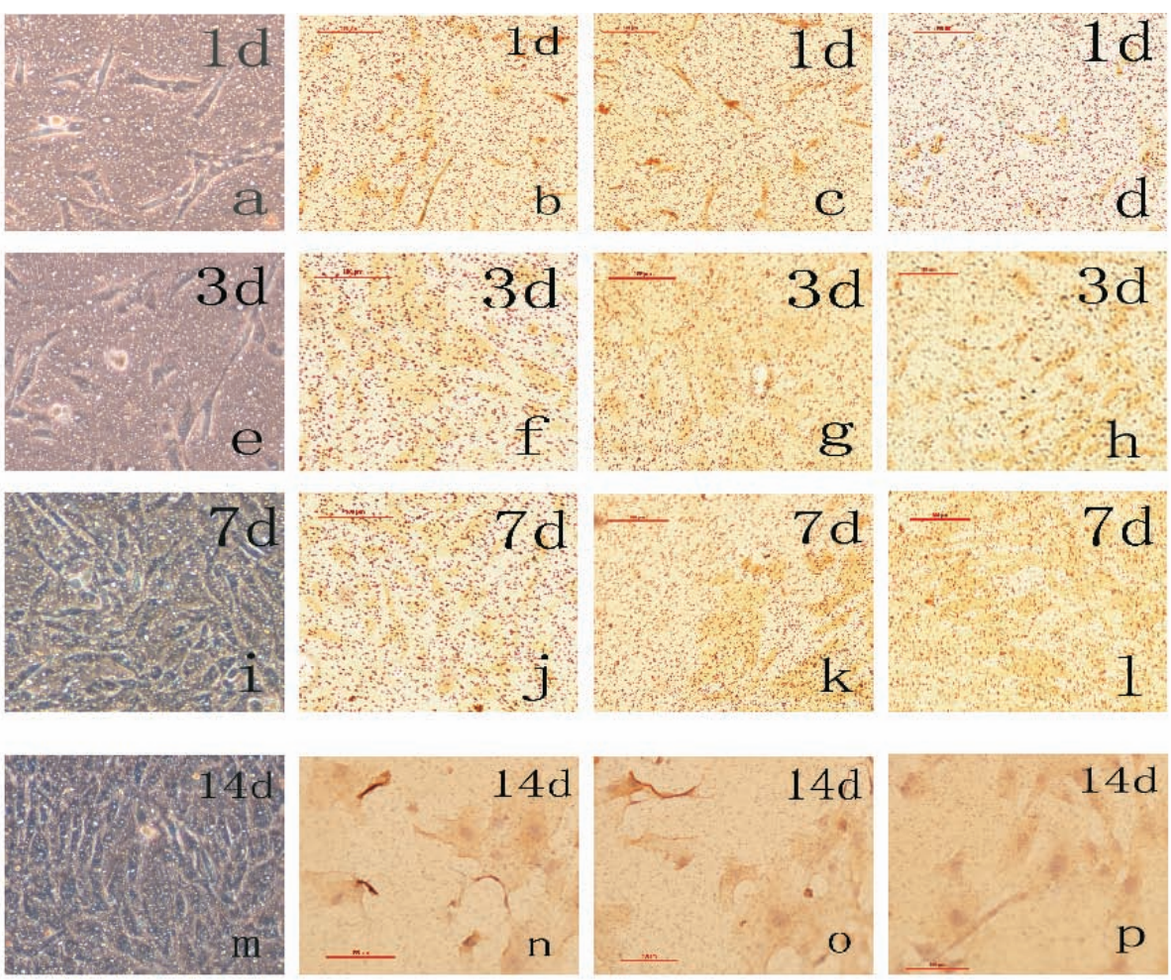

Fig. 3. Morphological and immunocytochemical assessments of co-cultured ADSCs. With respect to morphology, co-cultured ADSCs showed the elongated spindle shape characteristic of Schwann cells as early as 24 h after co-culture (a), while at 3, 7, and 14 days after co-culture, co-cultured ADSCs with that shape became more and more numerous (e, i, m). Immunocytochemical assessments of co-cultured ADSCs at different time points (1, 3, 7, 14 d) showed positive for S-100 (b, f, j, n), Nestin (c, g, k, o), and GFAP (d, h, l, p), but the percentage of positive cells could not be counted precisely because the transparency of the polycarbonate membranes was not good enough, so we could not perform precise quantitative analyses only on the basis of immunocytochemical pictures. Scale bar = 100 μm.

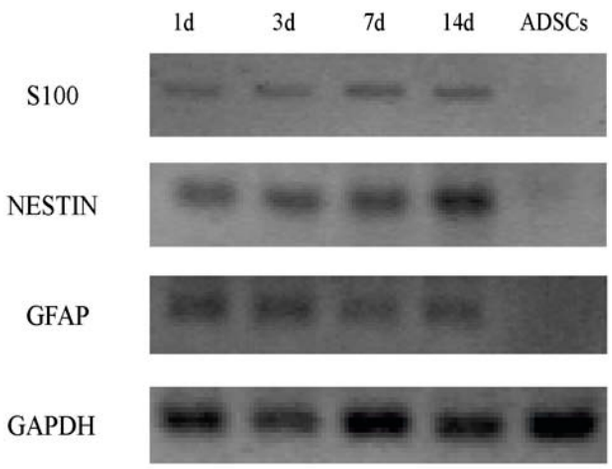

Fig. 4. Western blot analysis of Schwann cell-related proteins. Lyzates of co-cultured ADSCs at 1, 3, 7, and 14 days and lyzates of ADSCs from control groups were blotted for S100, Nestin, and GFAP proteins (GAPDH was used as a loading control).

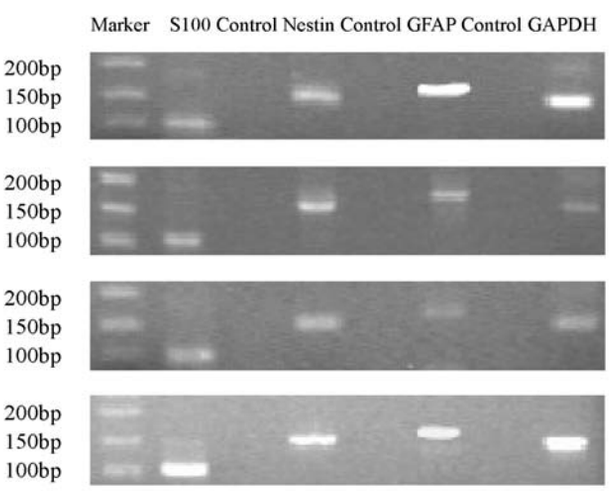

Fig. 5. RT-PCR gel electrophoresis images. In above figures, all the co-cultured ADSCs at 1, 3, 7, and 14 days show positive strips for gene S100, Nestin, and GFAP in different degrees, while the ADSCs from control groups show no positive strips for S100, Nestin, and GFAP. We use GAPDH as a reference for assessing the PCR efficiency.

Table 2. Relative differences in S100 gene expression. *Means for groups in homogeneous subsets are displayed. **Uses harmonic mean sample size = 3.000. Tukey HSD) Tukey's honestly significant difference test; Sig) significance.

	Time point (d)	N	Subset for alpha = .05	
			1*	2*
Tukey HSD**	1	3	.0000	
	3	3	.3010	
	7	3		3.3580
	14	3		4.5787
	Sig.		.750	.217

Table 3. Relative differences in Nestin gene expression. *Means for groups in homogeneous subsets are displayed. **Uses harmonic mean sample size = 3.000. Tukey HSD) Tukey's honestly significant difference test; Sig) significance.

	Time point (d)	N	Subset for alpha = .05	
			1*	2*
Tukey HSD**	3	3	.0000	
	1	3	.2188	
	7	3		4.5641
	14	3		4.7800
	Sig.		.995	.995

Table 4. Relative differences in GFAP gene expression. *Means for groups in homogeneous subsets are displayed. **Uses harmonic mean sample size = 3.000. Tukey HSD) Tukey's honestly significant difference test; Sig) significance.

	Time point (d)	N	Subset for alpha = .05
			1*
Tukey HSD**	1	3	.0000
	3	3	.7246
	7	3	1.2984
	14	3	1.4477
	Sig.		.058

for S-100, Nestin, and GFAP protein at all time points (1, 3, 7, 14 d), but the percentage of positive cells could not be counted precisely because the transparency of the polycarbonate membranes was not good enough, so we could not perform a precise quantitative analysis using only immunocytochemical pictures (Fig. 3). On the other hand, cultured ADSCs in the control groups kept their original small round or polygonal shape without changing to an elongated spindle shape, and these undifferentiated ADSCs showed negative for S-100, Nestin, and GFAP protein all the time. To confirm the results obtained by immunocytochemistry, Western blotting was performed (Fig. 4). Lyzates of co-cultured ADSCs at 1, 3, 7, and 14 days – but not ADSCs from the control groups – showed a GFAP-immunoreac-

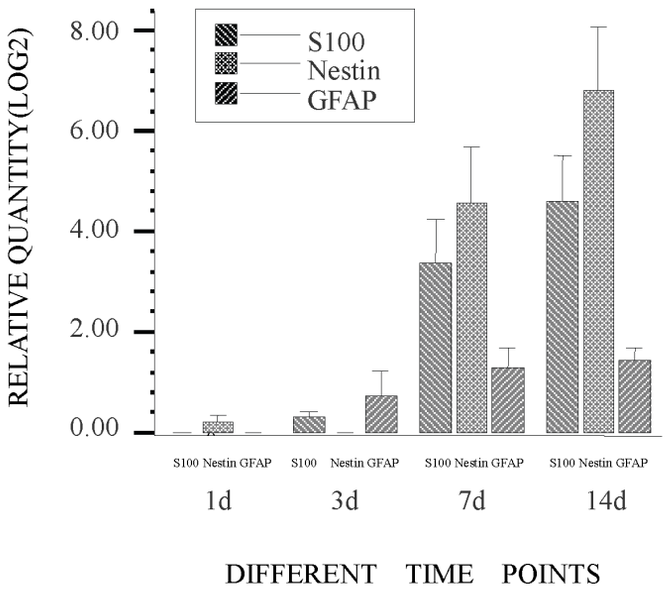

Fig. 6. Relative differences in S100, Nestin, and GFAP gene expression of co-cultured ADSCs. In the graph, bar height represents the relative quantity of gene expression (mean + SEM). For the relative quantities of S100 and Nestin gene expression, analyses showed no statistical differences between 1 and 3 d and between 7 and 14 d ($P > 0.05$), but the results for 7 or 14 d had significant statistical differences compared to those for 1 or 3 d ($P < 0.05$); for the relative quantities of GFAP gene expression, there were no statistical differences at 1, 3, 7, and 14 d ($P > 0.05$).

tive band corresponding to a molecular weight of 50 kDa. Nestin and S100 proteins were also detected in co-cultured ADSCs, but were absent in ADSCs from the control groups.

We also performed RT-PCR, and the results were consistent with immunocytochemistry and western blotting (Fig. 5). Subsequently, quantitative real-time PCR was performed to investigate the relative quantitative differences in gene expression of the above three genes at different time points (1, 3, 7, 14 d). For S100 and Nestin, analyses showed no statistical differences between 1 and 3 d and between 7 and 14 d ($P > 0.05$), but results for 7 and 14 d had significant statistical differences compared to those for 1 and 3 d ($P < 0.05$), which meant that the relative quantities of S100 and Nestin gene expression were higher at 7 and 14 d than at 1 and 3 d (Tables 2 and 3). For GFAP, there were no statistical differences at 1, 3, 7, and 14 d ($P > 0.05$), which meant that the relative quantity of GFAP gene expression maintained a stable level from 1 to 14 days without apparent fluctuation (Table 4). To make the results clear and direct, we used a bar graph to show relative quantitative differences at different time points (1, 3, 7, 14 d) for S100, Nestin, and GFAP (Fig. 6).

DISCUSSION

Our studies showed that ADSCs can differentiate into a Schwann cell phenotype only as a result of being co-cultured with SCs indirectly, excluding the possibility of cell fusion. Previous studies reported that BMSCs can be induced to undergo neural differentiation in the presence of certain cell growth factors such as BDNF, NGF, bFGF, PDGF, etc. (Sanchez et al., 2000; Tohill et al., 2004; Tao et al., 2005; Caddick et al., 2006). Recently, two papers reported that when supplemented with certain cell growth factor compounds, ADSCs can also be induced to differentiate into a Schwann cell phenotype (Kingham et al., 2007; Krampera et al., 2007). Adult SCs can secrete BDNF and NGF (Yamamoto et al., 1993), which makes it possible for stem cells to differentiate into neuro-like cells when co-cultured with SCs. Zurita et al. performed indirect co-culture of SCs and BMSCs in transwell culture dishes and demonstrated neural differentiation of BMSCs (Zurita et al., 2007). We observed that ADSCs began morphologic change as early as 1 day after co-culture, expressing S100, Nestin, and GFAP to judge from immunocytochemical staining and RT-PCR analysis, and such expressions lasted until two weeks later. These results showed that neurotrophic SC factors can induce rapid and stable neural differentiation of ADSCs, which is in keeping with previous research (Tao et al., 2005; Kingham et al., 2007; Zurita et al., 2007). On the basis of the above analyses, we believe that co-culture represents a simple and effective way of inducing neural differentiation of ADSCs.

In our studies, S100 protein, a special cell marker of Schwann cells, showed a relative quantity of gene expression that climbed from the 1st to 7th day, then remained stable until the 14th day. Nestin, a neural progenitor marker, exhibited the same regularity as S100 gene expression. As for GFAP, a glial marker, although we could see directly from the bar graph (Fig. 6) that the relative quantities of its gene expression increased continually from the 1st to 14th day,

there were no statistical differences between 1, 3, 7, and14 d. The S100 protein, Nestin, and GFAP are all recognized as cell surface markers of SCs (Zurita et al., 2005, 2007; Caddick et al., 2006; Kingham et al., 2007). Their strong gene expression in our co-cultured ADSCs indicated neural differentiation toward a Schwann cell phenotype. Analyzing the above results, we conclude that although ADSCs began neural differentiation as early as 1 day after co-culture, significant neural differentiation appeared at least 7 days later, and such differentiations can last at least two weeks. In other words, we needed at least 7 days to co-culture ADSCS with SCs *in vitro* before the co-cultured ADSCs could be transplanted into areas with peripheral nerve defects *in vivo* for nerve repair. Zurita et al. suggested previously that *in vitro* neural differentiation of BMSCs is unnecessary when BMSCs are used in grafting procedures for nervous system repair (Zurita et al., 2007). However, further investigation is needed to establish whether prior *in vitro* neural differentiation of ADSCs would be more effective for nerve repair *in vivo*.

Acknowledgments — This study was supported by funds from National Natural Science Foundation of China (No. 30772448). The work presented in this paper involves no conflicts of interest.

REFERENCES

Alvarez-Dolado, M., Pardal, R., Garcia-Verdugo, J. M., Fike, J. R., Lee, H. O., Pfeffer, K., et al. (2003). Fusion of bone-marrow-derived cells with Purkinje neurons, cardiomyocytes, and hepatocytes. *Nature* **425,** 968-973.

Bossolasco, P., Cova, L., Calzarossa, C., Rimoldi, S. G., Borsotti, C., Deliliers, G. L., et al. (2005). Neuro-glial differentiation of human bone marrow stem cells *in vitro*. *Exp. Neurol.* **193,** 312-325.

Caddick, J., Kingham, P. J., Gardiner, N. J., Wiberg, M., and *G. Terenghi* (2006). Phenotypic and functional characteristics of mesenchymal stem cells differentiated along a Schwann cell lineage. *Glia* **54,** 840-849.

Chen, K. A., Laywell, E. D., Marshall, G., Walton, N., Zheng, T., and *D. A. Steindler* (2006). Fusion of neural stem cells in culture. *Exp. Neurol.* **198,** 129-135.

Chopp, M., and *Y. Li* (2002). Treatment of neural injury with marrow stromal cells. *Lancet. Neurol.* **1,** 92-100.

Fraser, J. K., Wulur, I., Alfonso, Z., and *M. H. Hedrick* (2006). Fat tissue: an underappreciated source of stem cells for biotechnology. *Trends Biotechnol.* **24,** 150-154.

Gimble, J. M., Katz, A. J., and *B. A. Bunnell* (2007). Adipose-derived stem cells for regenerative medicine. *Circ. Res.* **100,** 1249-1260.

Hermann, A., Gastl, R., Liebau, S., Popa, M. O., Fiedler, J., Boehm, B. O., et al. (2004). Efficient generation of neural stem cell-like cells from adult human bone marrow stromal cells. *J. Cell Sci.* **117,** 4411-4422.

Kang, S. K., Lee, D. H., Bae, Y. C., Kim, H. K., Baik, S. Y., and *J. S. Jung* (2003). Improvement of neurological deficits by intracerebral transplantation of human adipose tissue-derived stromal cells after cerebral ischemia in rats. *Exp. Neurol.* **183,** 355-366.

Kingham, P. J., Kalbermatten, D. F., Mahay, D., Armstrong, S. J., Wiberg, M., and *G. Terenghi* (2007). Adipose-derived stem cells differentiate into a Schwann cell phenotype and promote neurite outgrowth *in vitro*. *Exp. Neurol.* **207,** 267-274.

Krampera, M., Marconi, S., Pasini, A., Galie, M., Rigotti, G., Mosna, F., et al. (2007). Induction of neural-like differentiation in human mesenchymal stem cells derived from bone marrow, fat, spleen, and thymus. *Bone* **40,** 382-390.

Mahmood, A., Lu, D., and *M. Chopp* (2004). Marrow stromal cell transplantation after traumatic brain injury promotes cellular proliferation within the brain. *Neurosurgery* **55,** 1185-1193.

Ning, H. X., Lin, G. T., Lue, T. F., and *C. S. Lin* (2006). Neuron-like differentiation of adipose tissue-derived stromal cells and vascular smooth muscle cells. *Differentiation* **74,** 510-518.

Safford, K. M., Hicok, K. C., Safford, S. D., Halvorsen, Y. D., Wilkison, W. O., Gimble, J. M., et al. (2002). Neurogenic differentiation of murine and human adipose-derived stromal cells. *Biochem. Biophys. Res. Commun.* **294,** 371-379.

Sanchez-Ramos, J., Song, S., Cardozo-Pelaez, F., Hazzi, C., Stedeford, T., Willing, A., et al. (2000). Adult bone marrow stromal cells differentiate into neural cells *in vitro*. *Exp. Neurol.* **164,** 247-256.

Tao, H., Rao, R. M., and *D. F. David* (2005). Cytokine-induced stable neuronal differentiation of human bone marrow mesenchymal stem cells in a serum/feeder cell-free condition. *Development Growth Differentiation* **47,** 423-433.

Tohill, M., Mantovani, C., Wiberg, M., and *G. Terenghi* (2004). Rat bone marrow mesenchymal stem cells express glial markers and stimulate nerve regeneration. *Neurosci. Lett.* **362,** 200-203.

Wang, X., Willenbring, H., Akkari, Y., Torimaru, Y., Foster, M., Al-Dhalimy, M., et al. (2003). Cell fusion is the principal source of bone-marrow-derived hepatocytes. *Nature* **422,** 897-901.

Woodbury, D., Schwarz, E. J., Prockop, D. J., and *I. B. Black* (2000). Adult rat and human bone marrow stromal cells differentiate into neurons. *J. Neurosci. Res.* **61,** 364-370.

Yamamoto, M., Sobue, G., Li, M., Arakawa, Y., Mitsuma, T., and *K. Kimata* (1993). Nerve growth factor (NGF), brain-derived neurotrophic factor (BDNF), and low-affinity nerve growth factor receptor (LNGFR) mRNA levels in cultured rat Schwann cells; differential time- and dose-dependent regulation by cAMP. *Neurosci. Lett.* **152,** 37-40.

Ying, Q. L., Nichols, J., Evans, E. P., and *A. G. Smith* (2002). Changing potency by spontaneous fusion. *Nature* **416,** 545-548.

Zuk, P. A., Zhu, M., Mizuno, H., Huang, J., Futrell, J. W., Katz, A. J., et al. (2001). Multilineage cells from human adipose tissue: implications for cell-based therapies. *Tissue Eng.* **7,** 211-228.

Zurita, M., and *J. Vaquero* (2004). Functional recovery in chronic paraplegia after bone marrow stromal cells transplantation. *Neuroreport* **15,** 1105-1108.

Zurita, M., and *J. Vaquero* (2006). Bone marrow stromal cells can achieve cure of chronic paraplegic rats: functional and morphological outcome one year after transplantation. *Neurosci. Lett.* **402,** 51-56.

Zurita, M., Vaquero, J., Oya, S., and *M. Miguel* (2005). Schwann cells induce neuronal differentiation of bone marrow stromal cells. *Neuroreport* **16,** 505-508.

Zurita, M., Vaquero, J., Oya, S., Bonilla, C., and *C. Aguayo* (2007). Neurotrophic Schwann-cell factors induce neural differentiation of bone marrow stromal cells. *Neuroreport* **18,** 1713-1717.